This article was downloaded by: *[CAS Chinese Academy of Sciences]*
On: *31 August 2009*
Access details: *Access Details: [subscription number 789038232]*
Publisher *Taylor & Francis*
Informa Ltd Registered in England and Wales Registered Number: 1072954 Registered office: Mortimer House, 37-41 Mortimer Street, London W1T 3JH, UK

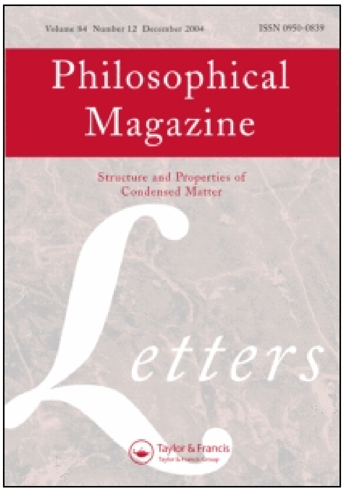

Philosophical Magazine Letters
Publication details, including instructions for authors and subscription information:
http://www.informaworld.com/smpp/title~content=t713695410

Networking amorphous phase reinforced titanium composites which show tensile plasticity

F. Q. Guo [ab]; S. J. Poon [a]; G. J. Shiflet [b]
[a] Department of Physics, University of Virginia, Charlottesville, VA, USA [b] Department of Materials Science and Engineering, University of Virginia, Charlottesville, VA, USA

Online Publication Date: 01 August 2008

To cite this Article Guo, F. Q., Poon, S. J. and Shiflet, G. J.(2008)'Networking amorphous phase reinforced titanium composites which show tensile plasticity',Philosophical Magazine Letters,88:8,615 — 622

To link to this Article: DOI: 10.1080/09500830802356739

URL: http://dx.doi.org/10.1080/09500830802356739

PLEASE SCROLL DOWN FOR ARTICLE

Full terms and conditions of use: http://www.informaworld.com/terms-and-conditions-of-access.pdf

This article may be used for research, teaching and private study purposes. Any substantial or systematic reproduction, re-distribution, re-selling, loan or sub-licensing, systematic supply or distribution in any form to anyone is expressly forbidden.

The publisher does not give any warranty express or implied or make any representation that the contents will be complete or accurate or up to date. The accuracy of any instructions, formulae and drug doses should be independently verified with primary sources. The publisher shall not be liable for any loss, actions, claims, proceedings, demand or costs or damages whatsoever or howsoever caused arising directly or indirectly in connection with or arising out of the use of this material.

Philosophical Magazine Letters
Vol. 88, No. 8, August 2008, 615–622

Networking amorphous phase reinforced titanium composites which show tensile plasticity

F.Q. Guo[a][b]*, S.J. Poon[a] and G.J. Shiflet[b]

[a]*Department of Physics, University of Virginia, Charlottesville, VA, USA;* [b]*Department of Materials Science and Engineering, University of Virginia, Charlottesville, VA, USA*

(*Received 27 May 2008; final version received 15 July 2008*)

Titanium matrix composites reinforced by an *in situ* formed networking amorphous phase have been prepared directly in the form of as-cast ingots. The composites show significant compressive and tensile plasticity. In contrast to the highly localized plasticity for most monolithic amorphous alloys, the tensile deformation of the current composites distributes uniformly over the entire specimen as a consequence of substantial work (strain) hardening. The formation mechanism of the networking structure, as a result of well-separated two-step solidification of the current alloy melts, have possible implications for composite synthesis in other alloy systems.

Keywords: Ti alloys; metallic glass; mechanical test; tensile plasticity

1. Introduction

Amorphous alloys can exhibit high yield and fracture strengths, large elastic strain and superior corrosion and wear resistance. In bulk form, this collection of properties are of particular interest for structural applications [1]. After decades of extensive research, synthesis of bulk metallic glasses in various metal systems has been achieved [2–11]. While making large size amorphous samples is no longer a central challenge, improvement of plasticity has become an increasing concern. Experimentally, monolithic amorphous alloys show very limited global plasticity, although, within the highly localized shear bands, significant plastic deformation can take place due to strain (work) softening and thermal softening [12]. Various approaches have been explored aiming to improve the general plasticity of amorphous alloys [13–15]. One of the approaches is to introduce a second phase (usually crystalline) into the amorphous matrix through either an external resource or by partial crystallization or precipitation [13]. This second phase acts as a barrier to hinder the rapid propagation of the shear bands and enables their interaction and multiplication, and thus avoiding an early failure of the sample tested. More recently, researchers showed that the plasticity of an originally brittle amorphous alloy can be significantly improved by surface shot peening treatment, which introduces a large number of surface generated shear bands and hence leads to a more uniform deformation [16]. However, the improvements of macroscopic plasticity have been limited to the cases of confined stress states, such as, compressive and bending tests, while the tensile test is

---

*Corresponding author. Email: fg7b@virginia.edu

ISSN 0950–0839 print/ISSN 1362–3036 online

DOI: 10.1080/09500830802356739
http://www.informaworld.com

a standard testing method used to evaluate structural materials intended for practical service. There are only a few publications reporting tensile test results for metallic glasses, and include Zr- and La-based alloys [17–19]. In the present work, a series of new Ti-based composites reinforced by a unique networking amorphous phase are reported, which show about 4% global plasticity especially under tensile testing.

2. Experiments

Commercial grade elements (with purities of 99.4% or higher) were used to produce the alloy ingots. Alloys with nominal compositions were prepared in an arc-furnace under a flowing argon atmosphere with a typical ingot weight of 15 g. Confirmation of the amorphous phase and the phase structures of the as-made ingots were carried out using an X-ray diffractometer (XRD) with CuKα radiation, a transmission electron microscope (TEM) operated at 200 kV and high resolution TEM (HRTEM) operated at 400 kV. Crystallization and melting behavior were studied using differential thermal analysis (DTA) and differential scanning calorimeter (DSC) at heating and cooling rates of 20°C min^{-1}. The center sections of the samples were used for all the above characterizations. Both compressive and tensile mechanical strength tests were done using a screw driven frame at strain rates of 10^{-4} s^{-1}. Compressive test specimens were cut directly from the as-cast ingots into rectangular blocks of about $2.5 \times 2.5 \times 5$ mm. For the tensile test, the as-cast ingots were first reshaped to finger-like and then machined to dog-bone shape with the gauge area dimension of 2.5×15 mm, and finally cut into thin slices of 0.5 mm in thickness. Specimens for both compressive and tensile tests were polished before testing.

3. Results and discussion

The synthesis of the current Ti composites is part of a continuous effort for improving Ti-based bulk amorphous alloys previously developed [11]. The Ti-based amorphous alloys exhibit excellent glass-forming ability, being able to form 'glass ingots' under normal cooling conditions, and display good compressive plasticity. However, there is no detectable plasticity observed in a tensile test. Improvement of the tensile plasticity will make these alloys more attractive for practical applications. Based on this goal, networking amorphous phase reinforced titanium matrix composites were prepared successfully, which reveal improved plasticity, especially under tensile loading stress.

Figure 1 shows the XRD patterns for three compositions with gradually reduced Be concentration levels. Figure 2a–c shows the optical microscope observation results for the same series of alloys, demonstrating the microstructural pattern evolution. The three alloys referred here are: Be10 ($Ti_{55}Zr_{30}Cu_5Be_{10}$, in at.%), Be5 ($Ti_{55}Zr_{35}Cu_5Be_5$) and Be2 ($Ti_{58}Zr_{35}Cu_5Be_2$). All three alloys show dominant crystalline diffraction peaks (Figure 1), which are indexed to be the β-titanium (bcc) solid solution phase. When compared to pure β titanium, the diffraction peaks of the current β solid solution shift to lower angles due to the solubility of zirconium. The relative intensity of a diffuse diffraction signal from the amorphous phase decreases with reduced Be contents, indicating less amorphous phase volume fraction. Optical microscopy (OM) observation of Be10 (Figure 2a) reveals a uniform networking structure, with the cell size of about 5 μm. Be5 (Figure 2b) has a similar networking structure but the cell size increases to about 15 μm, and

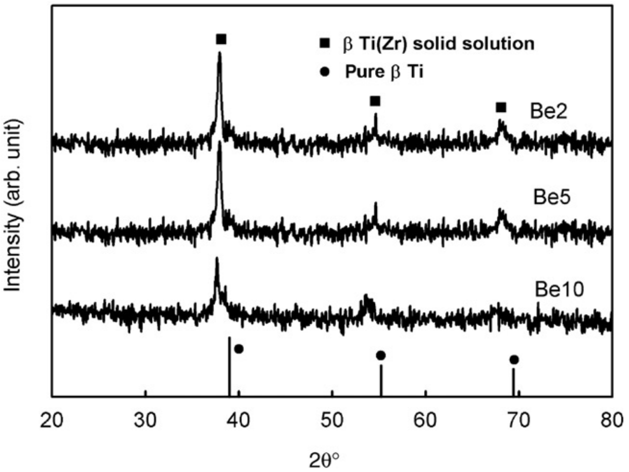

Figure 1. XRD patterns of as-made alloy ingots, where Be10, Be5, and Be2 represent $Ti_{55}Zr_{30}Cu_5Be_{10}$, $Ti_{55}Zr_{35}Cu_5Be_5$, and $Ti_{60}Zr_{33}Cu_5Be_2$, respectively.

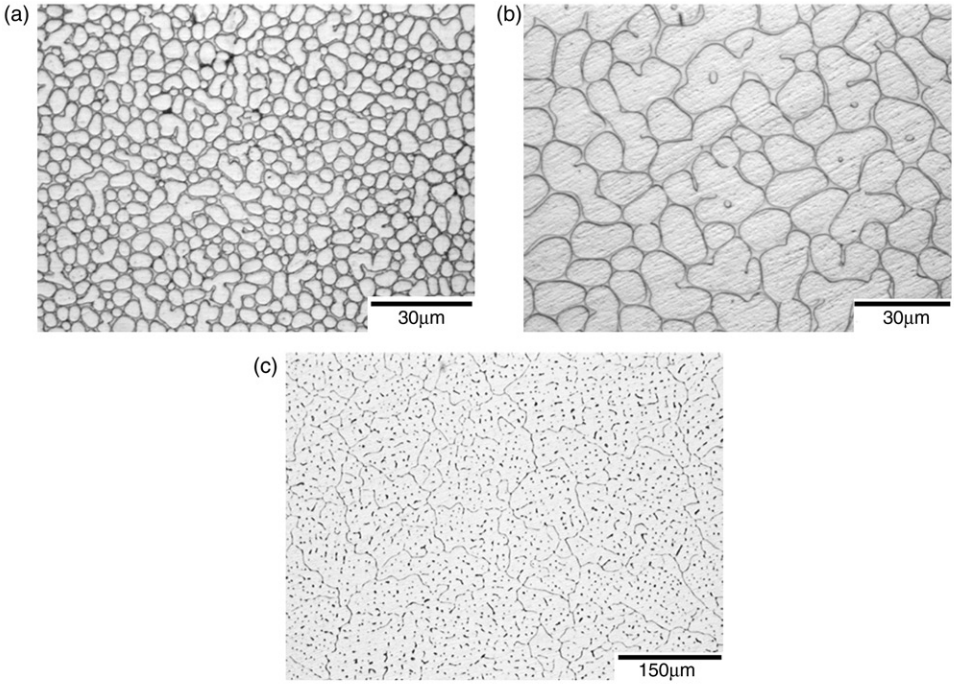

Figure 2. Optical microscopy images of as-made alloy ingots, where (a), (b), and (c) are for alloy Be10, Be5, and Be2, respectively.

at the same time, the networking is occasionally disconnected. While for Be2 (Figure 2c) most of the networking becomes disconnected, the networking pattern evolves into discontinuous rods and particles. However, under a lower magnification, there still exists a networking-like structure with the cell size having a much larger scale of ~200 μm. The volume fraction of the networking phase (i.e. amorphous phase, as verified from TEM, discussed later) was estimated to be around 50, 30, and 10% for alloys Be10, Be5, and Be2, respectively, by assuming that the volume fraction can be represented by the percentage of the area of the networking phase occupied in the OM images shown in Figure 2.

Transmission electron microscope observations, shown for alloy Be10 (Figure 3a), clarifies that the networking structure is an amorphous phase, characterized by the mottled pattern in the HRTEM image (Figure 3b) and its distinctive halo rings from electron diffraction (Figure 3b, inset). While the near-spherical cells, which are surrounded by the networking amorphous phase, are β titanium, confirmed by the HRTEM image in

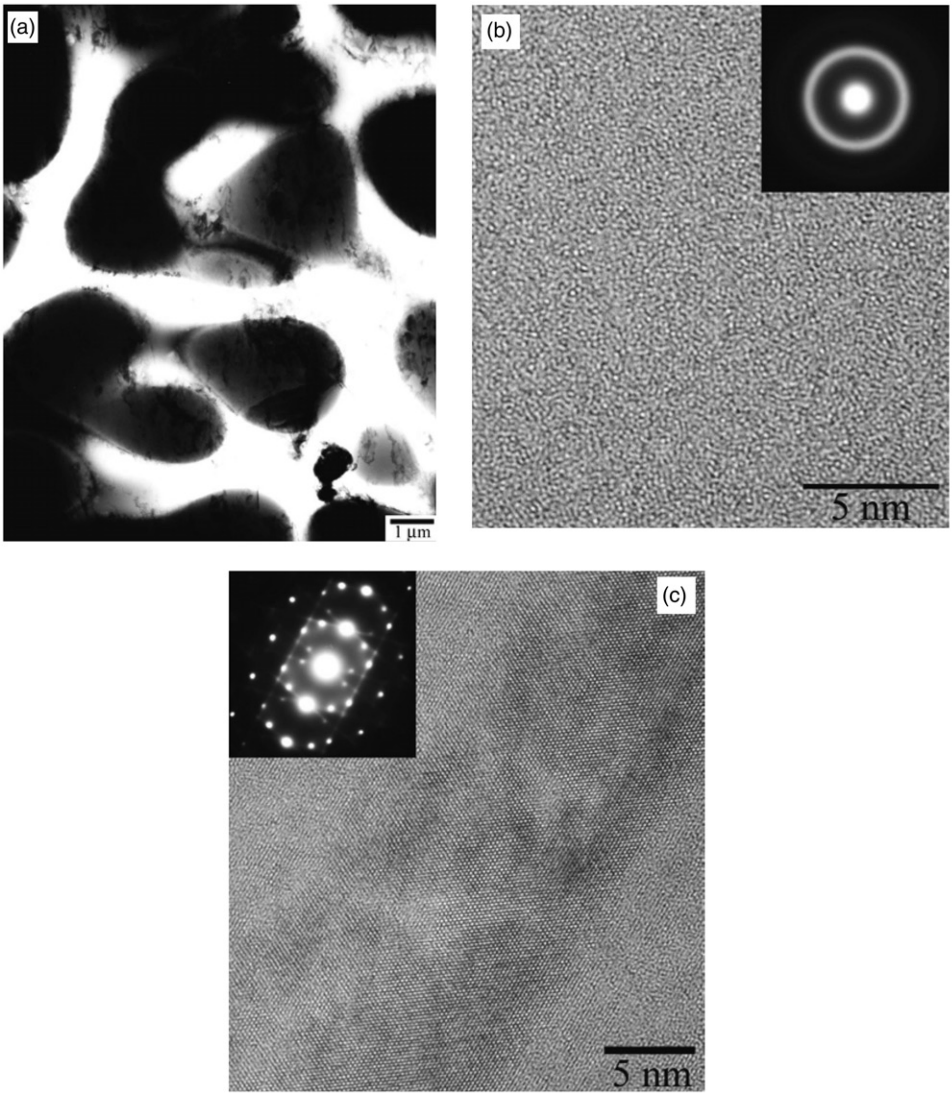

Figure 3. TEM image (a) illustrating the two-phase structure of alloy Be10 and HRTEM images to reveal the amorphous network (b) and BCC β phase (c).

Figure 3c and the (inset) diffraction pattern. Every crystalline cell is a single grain for alloys Be10 and Be5, confirmed by both OM and HRTEM observations. Chemically etched OM samples do not show any evidence of grain boundaries inside the cell. HRTEM observation demonstrates that the lattice orientation remains the same within a single cell.

Tensile stress–strain testing was done on the Be5 alloy; results are shown in Figure 4. Both engineering stress–strain and true stress–true strain curves demonstrate that the alloy sustains ~4% plastic deformation before final fracture, with remarkable work (strain) hardening effect. Accompanied with the work hardening effect, uniform plastic deformation was observed during the tensile testing. Figure 5a shows an OM picture of the Be5 alloy fractured after tensile loading. The plastic deformation is distributed uniformly over the whole gauge length. The surface within the gauge length becomes rumpled and uneven when compared with the neighboring shoulder areas at both ends. A higher magnification OM observation shown in Figure 5b reveals, interestingly, that the deformation shear bands start and end away from the specimen edges. The orientation of the shear bands distribute randomly. If a neighborhood of shear bands which shares the

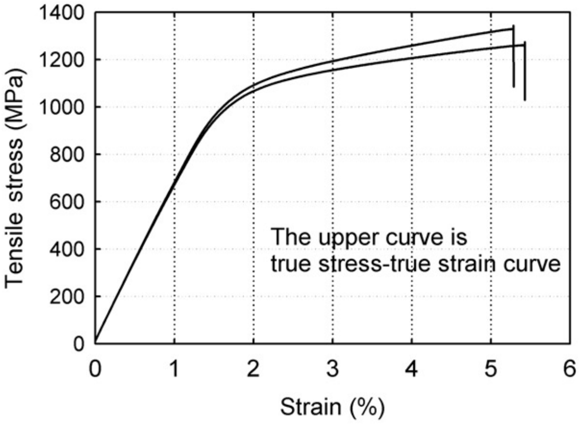

Figure 4. Tensile stress–strain curves for the Be5 alloy.

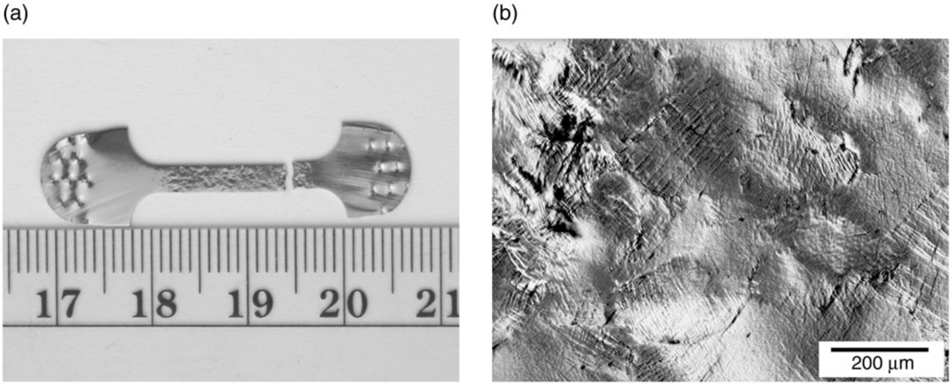

Figure 5. OM image (a) of the specimen surface after tensile fracture and SEM image (b) of the surface details of the fractured specimen for alloy Be5.

same orientation is referred to as a group, then the size of a shear band group is in the range of 200 μm or larger, greater than the networking cell size for this particular alloy composition (~15 μm), indicating that the deformation propagates through the amorphous–crystalline interface.

To the authors' knowledge, this is the first report of the formation of a networking amorphous phase structure. Since this particular structure shows attractive mechanical properties, especially under tensile testing, it is important to explore the mechanism of the networking formation of the current alloys which then might have general implications for other alloy systems. Figure 6a gives the DTA curves for alloys Be10, Be5, and Be2, also given for comparison are the curves for the bulk glass former $Ti_{40}Zr_{25}Cu_{12}Ni_{3}Be_{20}$ and crystalline $Ti_{65}Zr_{35}Cu_{5}$. Alloys Be10 and Be5 have a clear crystallization reaction (near 450°C) indicating the existence of a prior amorphous phase while the crystallization heat released is small for alloy Be2 because of its much lower initial amorphous phase volume fraction. In terms of melting, the endothermic signal in the range of 600–700°C is not entirely from the melting reaction of the alloys, one of the peaks is a result of the β-Ti solid state phase transformation. XRD patterns of the alloy $Ti_{62}Zr_{33}Cu_{5}$ (Figure 6b) indicate that a phase transformation from the as-made β (bcc) structure to the α (hcp) phase takes place, which occurs over a broad temperature range. Because the $\beta \rightarrow \alpha$ transformation is extended in this fashion, it explains why no distinct heat release signal is observed (Figure 6a).

Furthermore, although the endothermic signal related to a melting process at higher temperatures cannot be clearly defined in the ternary alloy, melting begins between 600°C and 700°C, but is not completed within this range for alloys Be10, Be5, and Be2, since the samples did not change their shape physically after heating to temperatures as high as 750°C. However, the bulk glass-forming sample $Ti_{40}Zr_{25}Cu_{12}Ni_{3}Be_{20}$ did change to a spherical shape at this temperature, indicating that it was fully melted. By heating the remaining alloy samples to even higher temperatures and using the physical change of their shape as the indication of final melting, it was found that for alloys Be10, Be5, and Be2 this occurs near 1080°C, 1150°C, and 1260°C, respectively. For the reference alloy $Ti_{62}Zr_{33}Cu_{5}$, the final melting is believed to be above 1300°C, since heating to 1300°C did not change the shape of the rectangular sample. Therefore, the current alloys

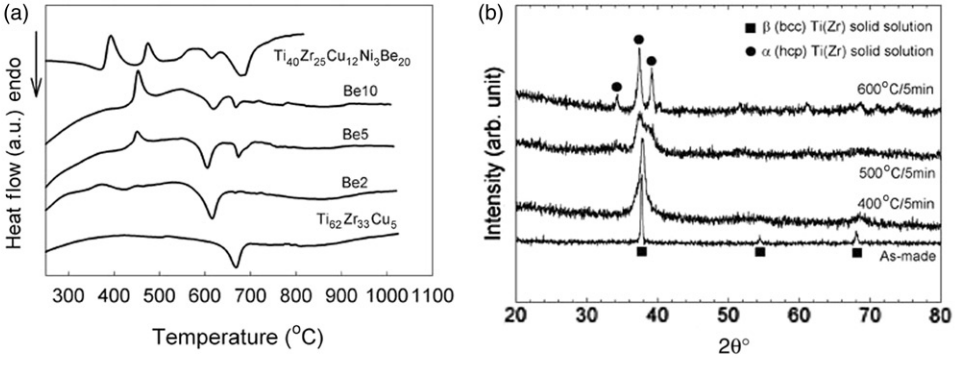

Figure 6. (a) DTA curves of the alloys Be10, Be5, and Be2, also given, for comparison, are curves for bulk glass former $Ti_{40}Zr_{25}Cu_{12}Ni_{3}Be_{20}$ and Be-free crystalline alloy $Ti_{62}Zr_{33}Cu_{5}$; (b) XRD pattern of as-made $Ti_{62}Zr_{33}Cu_{5}$ and patterns following heat treatment at different temperatures for 5 min.

melt (or solidify) in a well-separated two-step process, with the initial and final melting (solidification) temperature gap as large as 400–600°C. This feature of the current alloys is similar to Al-based amorphous alloys that have the initial and final melting (solidification) temperature gap of 200–300°C [20]. However, in the case of Al alloys the alloy compositions are hypereutectic, the solidification at higher temperatures involves the precipitation of Al compounds which requires substantial solute element partitioning, and hence is easily suppressed kinetically by applying a relatively high cooling rate on the alloy melt. If the formation of Al compound(s) is not suppressed, the precipitation of Al compounds would consume and thereby deplete solute constituents from the remaining liquid. This would consequently drive the liquid composition away from the optimal glass-forming composition and towards pure aluminium. However, it is different for the current Ti alloys, which are actually developed from the eutectic alloy $Ti_{40}Zr_{25}Cu_{12}Ni_3Be_{20}$ [11]. By introducing more matrix-solvent components (Ti as well as Zr, as they are inter-soluble and form an unlimited solid solution) at the expense of the solute constituents (Ni, Cu, and Be), the current Ti alloys are substantially hypoeutectic in chemical composition. As a result, β-Ti solid solution will precipitate first from the melt upon solidification. The precipitation of β-Ti solid solution is difficult to suppress even with a high cooling rate applied since it is favorable to take place both thermodynamically and kinetically. As confirmed in the case of melt spinning, where the cooling rate is in the range of 10^{6}°C s^{-1}, the formation of β-Ti solid solution still cannot be avoided for this composition. In association with the precipitation of β-Ti solid solution, glass formation is facilitated by the rejected solute constituents (Cu, Ni, and Be are because of their limited solubility in β-Ti solid solution, but Zr is soluble and not partitioned) thereby leading to the remaining liquid becoming enriched in these elements and moving closer to the (near) eutectic bulk glass-forming compositions. Therefore, the β-Ti solid solution precipitation is not required to be suppressed in order for the alloy to form some amorphous structure; it is in fact an essential step for the current alloys to form a networking amorphous phase. However, an adequate cooling rate should be achieved to make sure the remaining liquid freezes amorphously, which for the current alloys is estimated to be $\sim$100°C s^{-1}, based on the observation that they can be produced when cooling on the copper plate after arc melting. This formation mechanism should be applicable to other alloy systems, where good glass formability is available and the solute constituents have only limited solubility in the solvent matrix.

4. Conclusion

In summary, networking amorphous phase reinforced Ti composites were prepared in the form of as-cast alloy ingots. The composites show $\sim$4% tensile plasticity with uniform distributed deformation over the entire specimen. The well-separated two-step melting process, with the initial and final melting temperature gap of 400–600°C, is responsible for the networking formation in the current Ti alloys.

Acknowledgement

Research supported by DARPA Structural Amorphous Metals Program under ONR Grant No. N00014-06-1-0492 is acknowledged.

References

[1] J. Eckert, J. Das, S. Pauly et al., J. Mater. Res. 22 (2007) p.285.
[2] T. Zhang, A. Inoue and T. Masumoto, Mater. Trans. JIM 32 (1991) p.1005.
[3] A. Peker and W.L. Johnson, Appl. Phys. Lett. 63 (1993) p.2342.
[4] H. Ma, E. Ma and J. Xu, J. Mater. Res. 18 (2003) p.2288.
[5] V. Ponnambalam, S.J. Poon and G.J. Shiflet, J. Mater. Res. 19 (2004) p.1320.
[6] A. Inoue, W. Zhang, T. Zhang et al., Acta Mater. 49 (2001) p.2645.
[7] F.Q. Guo, S.J. Poon and G.J. Shiflet, Appl. Phys. Lett. 83 (2003) p.2575.
[8] D.H. Xu, G. Duan and W.L. Johnson, Phys. Rev. Lett. 92 (2004) p.245504.
[9] N. Nishiyama and A. Inoue, Mater. Trans. JIM 37 (1996) p.1531.
[10] Y.C. Kim, W.T. Kim and D.H. Kim, Mater. Sci. Engi. A 375–377 (2004) p.127.
[11] F.Q. Guo, H-J. Wang, G.J. Shiflet et al., Appl. Phys. Lett. 86 (2005) p.091907.
[12] J.J. Lewandowski and A.L. Greer, Nat. Mater. 5 (2006) p.15.
[13] C.C. Hays, C.P. Kim and W.L. Johnson, Phys. Rev. Lett. 84 (2000) p.2901.
[14] J. Eckert, U. Kuhn, N. Mattern et al., Intermetallics 10 (2002) p.1183.
[15] H. Ma, J. Xu and E. Ma, Appl. Phys. Lett. 83 (2003) p.2793.
[16] Y. Zhang, W.H. Wang and A.L. Greer, Nat. Mater. 5 (2006) p.857.
[17] R.D. Conner, R.B. Dandliker and W.L. Johnson, Acta Mater. 46 (1998) p.6089.
[18] F. Szuecs, C.P. Kim and W.L. Johnson, Acta Mater. 49 (2001) p.1507.
[19] F.Q. Guo, S.J. Poon and G.J. Shiflet, Mater. Sci. Forum 331 (2000) p.31.